GLRC_HEGIS : homogeneous reinforced concrete behaviour for shells

11th MFRONT User Day

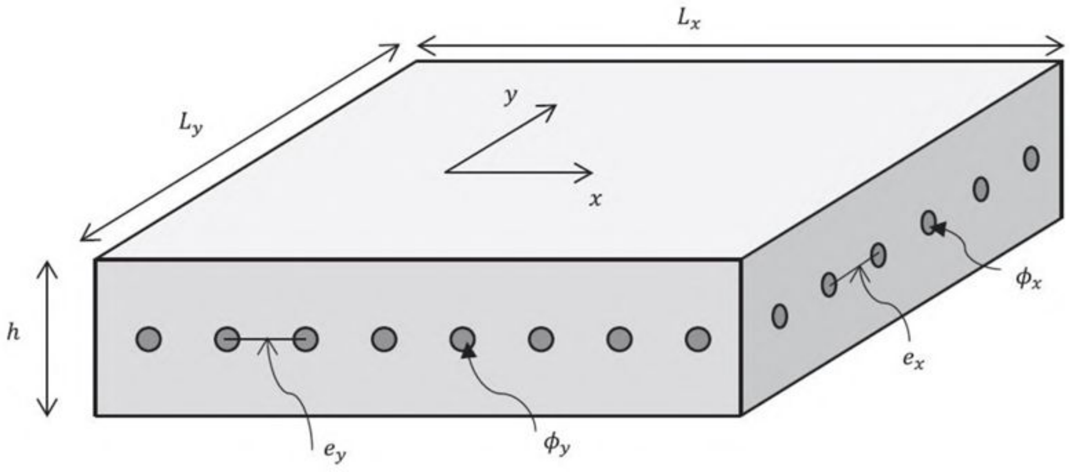

Autor : Lucas Turgne
Co-authors : Miquel Huguet & Olivier Lherminier

20/11/2025

Data sensitivity - Public

1 / CONTEXT – BACKGROUND

GLRC_HEGIS :

- Constitutive model for **homogenised reinforced concrete on shell elements** ;
- **4 dissipative** phenomena represented;
- Enables **accurate physical description** of reinforced concrete behaviour for monotonic and **cyclic loads** ;
- Extension of nuclear installations

Why implement the GLRC_HEGIS constitutive law in MFront ?

2016

Thesis by Miquel Huguet in collaboration with EDF, EGIS and Ecole Centrales de Nantes

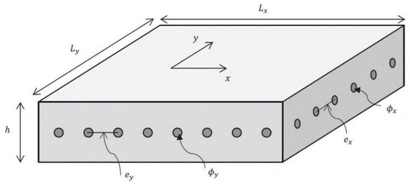

*1 : RVE RC Panel

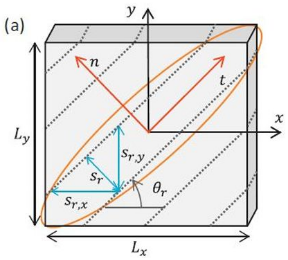

*3 : RVE RC Panel – cracking scheme

2020

Continuous improvement of the constitutive model ; Olivier Lherminier's second thesis to add out-of-plane non-linear behaviour

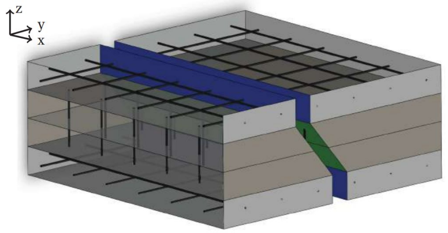

*2 : Out-of-plane cracking scheme

code_aster

Limitations :

- Improve convergence
- Use GLRC_HEGIS with ANSYS
- Learn how to use the MFront tool

2024

End-of-studies internship: implementation of the GLRC_HEGIS law on **MFront**

ANSYS

code_aster

Cast3M

*1 : M. HUGUET, Un modèle global homogénéisé pour la fissuration des voiles en béton armé sous chargements sismiques (2016)
*2 : O.LHERMINIER, thèse doctorale (2020)
*3 M. HUGUET & al. Stress resultant nonlinear constitutive model for cracked reinforced concrete panels (2017)

1 / GLRC_HEGIS – OVERWIEW

The GLRC_HEGIS non-linear constitutive model is a model of homogenised reinforced concrete shells that can be used to represent the behaviour of walls and floors outside the elastic range.

4 dissipative mechanical phenomena are modelled :

- **Damage to concrete** under compression ;
- **Cracking** of concrete ;
- **Relative slippage** between steel layers and concrete ;
- **Yielding of steel** layers

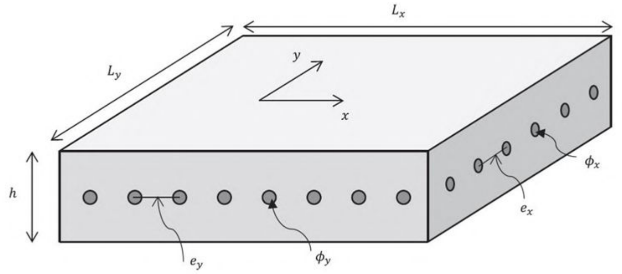

*1 : RVE RC Panel

Other consitutive models exist but do not represent physics as accurately ; these are damaging laws (Code_Aster) :

Multilayer shells :

- ENDO_ISOT_BETON + GRILLE_CINE_LINE
- BETON_REGLE_PR + GRILLE_CINE_LINE

Single-layer shells:

- GLRC_DM
- GLRC_DAMAGE
- DHRC

*1 : M. HUGUET, Un modèle global homogénéisé pour la fissuration des voiles en béton armé sous chargements sismiques (2016)

1 / CONTEXT - MOTIVATION

SMART 2013 mock-up, CEA-Saclay (France)

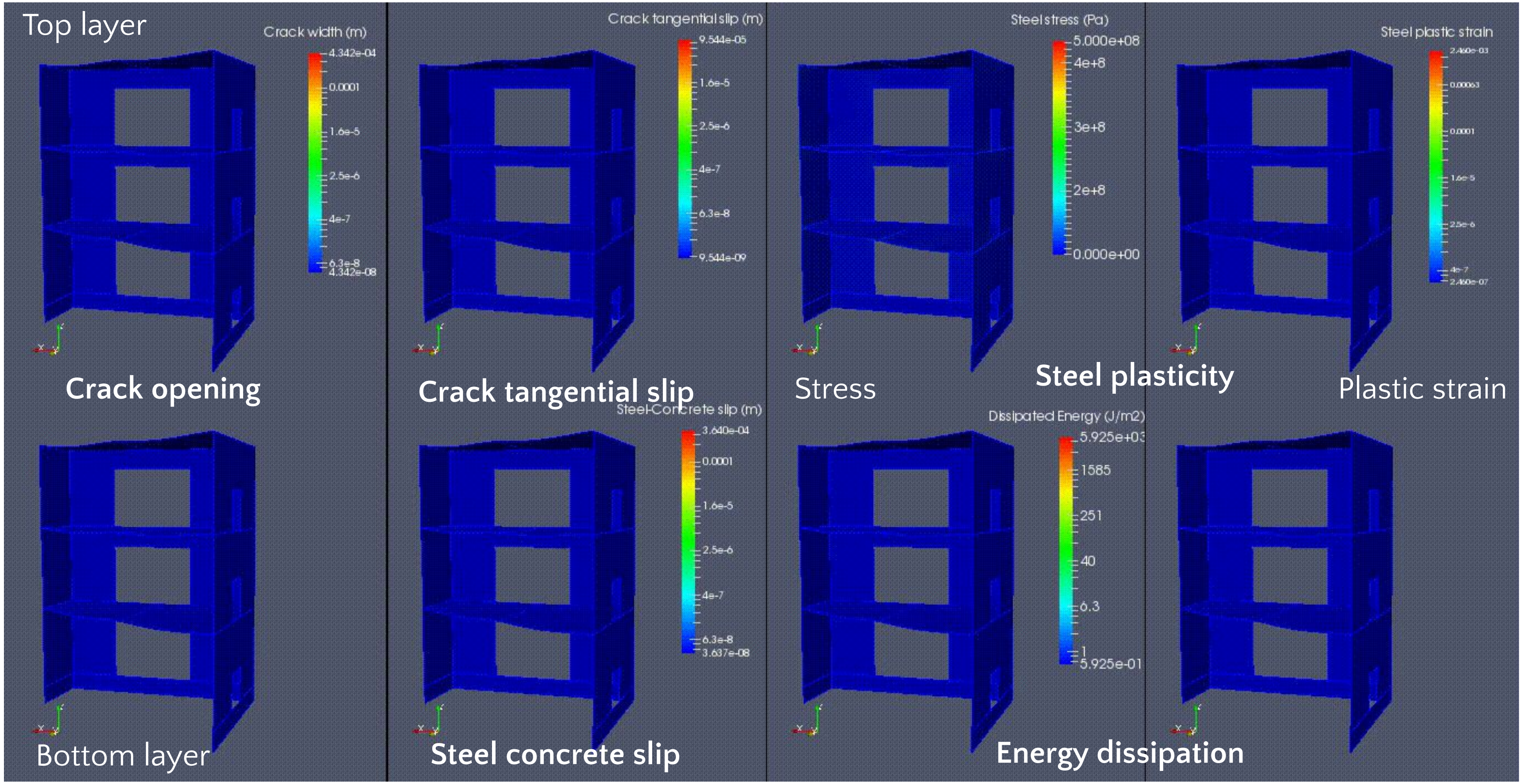

egis

Data sensitivity - Public

1 / GLRC_HEGIS – BEHAVIOUR OF CONCRETE UNDER COMPRESSION AND TENSION

Concrete damage : This reflects microcracking in concrete under compression via scalar variable ***d***. Plastic flow occurs beyond the elastic limit *fc*.

$$\begin{pmatrix}\sigma^c_{xx}\\ \sigma^c_{yy}\\ \sigma^c_{xy}\end{pmatrix} = \frac{E_c.\chi(d)}{1-\nu_c^2}\begin{pmatrix}1 & \nu_c & 0\\ \nu_c & 1 & 0\\ 0 & 0 & 1-\nu_c\end{pmatrix}\begin{pmatrix}\varepsilon^c_{xx}\\ \varepsilon^c_{yy}\\ \varepsilon^c_{xy}\end{pmatrix} \quad \text{avec} \quad \chi(d) = \frac{1+\gamma_d d}{1+d}$$

- Post-peak elastic slope : $\gamma_d E_c$
- Slope of discharge or recharge after damage : $\chi(d)E_c$

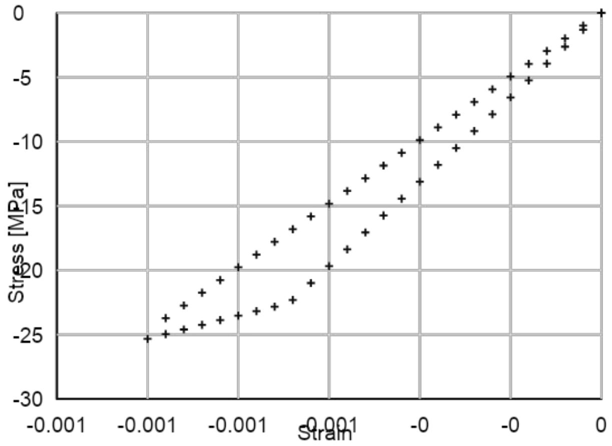

Stress – strain curve for damage concrete

Concrete cracking : When the principal stress exceeds the tensile strength of concrete *fct*, a crack appears. The two internal variables are summarised by the vector : $\mathbf{w_i} = (\mathbf{w_{i,n}}, \mathbf{w_{i,t}})$

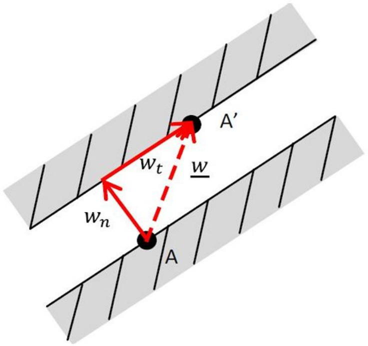

*1 : Crack opening scheme

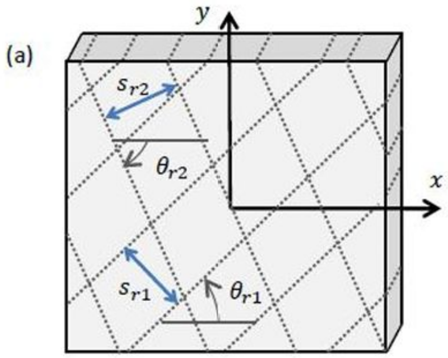

*1 : RVE RC Panel – two cracks scheme

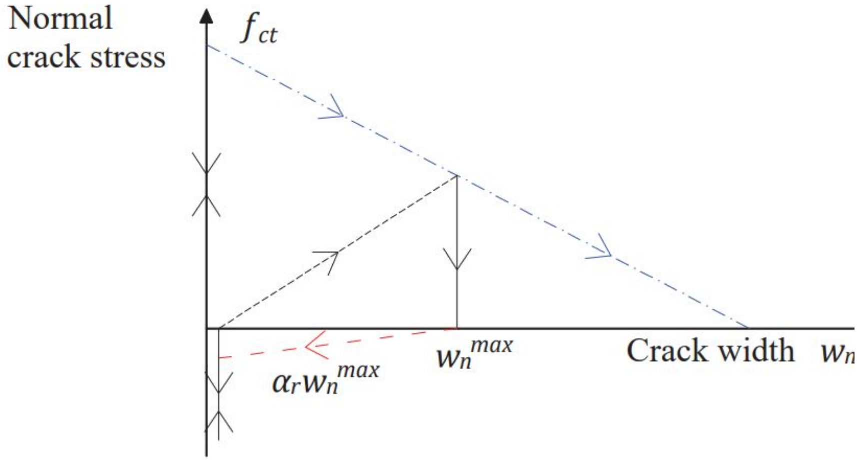

1* : Normal-to crack concrete stress at cracks as a function of crack opening

*1 : M. HUGUET, Un modèle global homogénéisé pour la fissuration des voiles en béton armé sous chargements sismiques (2016)

1 / GLRC_HEGIS – BEHAVIOUR OF STEEL-CONCRETE INTERACTION AND STEEL LAYERS

Relative steel/concrete slip: When concrete cracks, the tangential stresses at the interface between the two materials increase and are dependent on the displacement induced by the cracking. When these stresses become too high, the steel slips relative to the concrete. This irreversible displacement is represented by the internal vector variable $\underline{\boldsymbol{v}^p} = (\boldsymbol{v}_x^p, \boldsymbol{v}_y^p)$

$$\boxed{\underline{\tau} = \underset{\sim}{K}^{\tau}.(\underline{v} - \underline{v}^p) = \underset{\sim}{K}^{\tau}.(\underset{\sim}{M}^{vw}(\theta_r).\underline{w} - \underline{v}^p)}$$

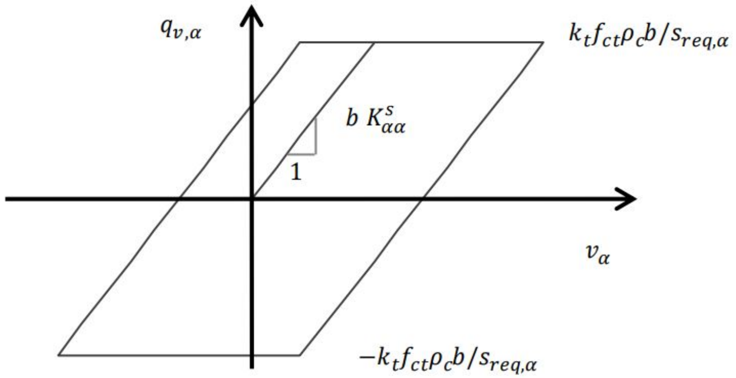

1* : Evolution of the slip thermodynamic force as a function of the concrete-steel slip

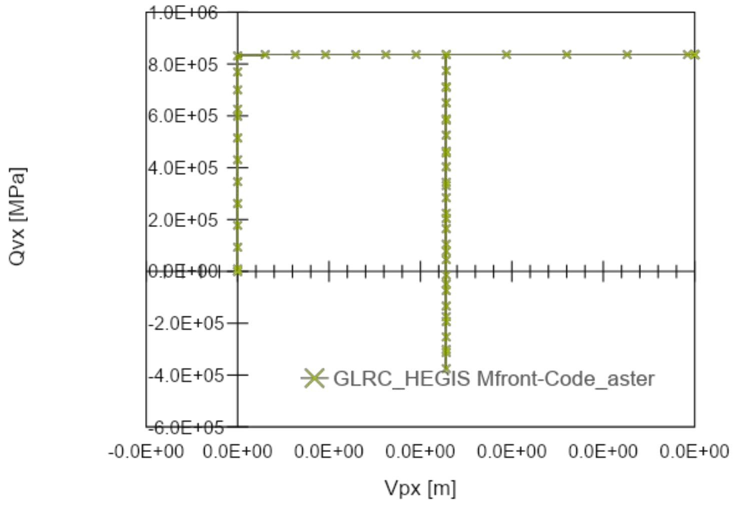

Yielding of steel layers : Locally, stresses in steels can be expressed using a perfectly plastic elastic law. When stresses exceed the limit fsy, the internal plastic variables change: $\underline{\boldsymbol{\varepsilon}^{ps}} = (\boldsymbol{\varepsilon}_x^{ps}, \boldsymbol{\varepsilon}_y^{ps})$

$$\boxed{\underset{\sim}{\sigma}^{s\alpha} = E_s(\varepsilon^s_{\alpha\alpha} - \varepsilon^{ps}_{\alpha\alpha})\underline{e}_\alpha \otimes \underline{e}_\alpha}$$

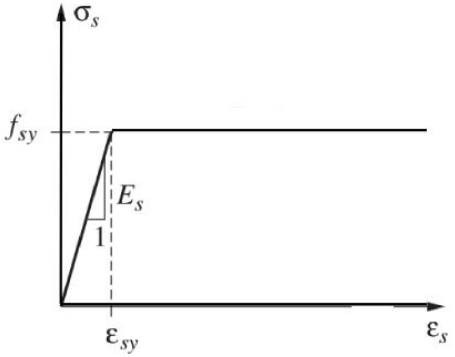

*1 : M. HUGUET, Un modèle global homogénéisé pour la fissuration des voiles en béton armé sous chargements sismiques (2016)

1 / GLRC_HEGIS – THERMODYNAMIC FORMULATION

To formulate the global model, we use the framework of the Thermodynamics of Isothermal Irreversible Processes, where the state of the material is defined by the Helmholtz free energy density: $\Psi(\underset{\sim}{\varepsilon}, \underline{\alpha})$

The material is then described by state and internal variables. The evolution of these variables is defined by the equations:

$$\underset{\sim}{N} = \frac{\partial \Psi_0(\underset{\sim}{\varepsilon}, \underline{\alpha})}{\partial \underset{\sim}{\varepsilon}} \quad \& \quad -q_i := \frac{\partial \Psi_0(\underset{\sim}{\varepsilon}, \underline{\alpha})}{\partial \alpha_i}$$

$$\Psi_m^\circ = \Psi_m^\circ(\boldsymbol{\varepsilon}, \boldsymbol{\gamma}, \underline{w}_\chi^\beta, \underline{v}^{p,\beta}, \underline{\epsilon}^{ps,\beta}, d^\beta)$$

$$= \boxed{\frac{1}{2}\boldsymbol{\varepsilon} : \mathbb{A}^\beta(d^\beta) : \boldsymbol{\varepsilon}} \boxed{- \sum_{\chi=1,2} \boldsymbol{\varepsilon} : \mathbb{B}_\chi^\beta(d^\beta) \cdot \underline{w}_\chi^\beta} + \sum_{\chi=1,2} \boldsymbol{\varepsilon}^{cd}(d^\beta) : \mathbb{B}_\chi^\beta(d^\beta) \cdot \underline{w}_\chi^\beta \boxed{- \boldsymbol{\varepsilon} : \mathbb{C}^\beta \cdot \underline{\epsilon}^{ps\beta}} + \sum_{\chi=1,2} \frac{1}{2} \underline{w}_\chi^\beta \cdot \mathbf{D}_\chi^\beta(d^\beta) \cdot \underline{w}_\chi^\beta \boxed{+ \frac{1}{2} \underline{v}^{p\beta} \cdot \mathbf{E}^\beta(d^\beta) \cdot \underline{v}^{p\beta}} + \frac{1}{2} \underline{\epsilon}^{ps\beta} \cdot \mathbf{F}^\beta \cdot \underline{\epsilon}^{ps\beta} - \sum_{\chi=1,2} \underline{w}_\chi^\beta \cdot \mathbf{G}_\chi^\beta(d^\beta) \cdot \underline{v}^{p\beta} + \underline{w}_1^\beta \cdot \mathbf{H}^\beta(d^\beta) \cdot \underline{w}_2^\beta$$

Elastic+damage **Cracking** **Steel yielding** **Steel-concrete sliding**

$$\mathbb{A}^\beta(d^\beta) = b^\beta \left(\rho_c^\beta \mathbb{C}_c(d^\beta) + \sum_\alpha \rho_{s\alpha}^\beta E_{s\alpha} \underline{e}_\alpha \otimes \underline{e}_\alpha \otimes \underline{e}_\alpha \otimes \underline{e}_\alpha \right)$$

$$\mathbb{B}_\chi^\beta(d^\beta) = b^\beta \rho_c^\beta \mathbb{C}_c(d^\beta) : \mathbb{M}^{\epsilon w}(\theta_{r,\chi})$$

$$\mathbb{C}^\beta = \sum_\alpha b^\beta \rho_{s\alpha}^\beta E_{s\alpha} \underline{e}_\alpha \otimes \underline{e}_\alpha \otimes \underline{e}_\alpha$$

$$\mathbb{I}^\beta(d^\beta) = b^\beta \rho_c^\beta \mathbb{C}_c(d^\beta)$$

$$\mathbf{D}_\chi^\beta = b^\beta \rho_c^\beta (\mathbb{M}^{\epsilon w}(\theta_{r,\chi}))^t : \mathbb{C}_c(d^\beta) : \mathbb{M}^{\epsilon w}(\theta_{r,\chi}) + (\mathbb{M}_\chi^{vw,\beta})^t \cdot \boldsymbol{K}^s(d^\beta) \cdot \mathbb{M}_\chi^{vw,\beta}$$

$$\mathbf{E}^\beta = \boldsymbol{K}^s(d^\beta)$$

$$\mathbf{F}^\beta = \sum_{\alpha=x,y,z} b^\beta \rho_{s\alpha}^\beta E_{s\alpha} \underline{e}_\alpha \otimes \underline{e}_\alpha$$

$$\mathbf{G}^\beta = (\mathbb{M}_\chi^{vw,\beta})^t \cdot \boldsymbol{K}^s(d^\beta)$$

$$\mathbf{H}^\beta = b^\beta \rho_c^\beta (\mathbb{M}^{\epsilon w}(\theta_{r,1}))^t : \mathbb{C}_c(d^\beta) : \mathbb{M}^{\epsilon w}(\theta_{r,2}) + (\mathbb{M}_1^{vw,\beta})^t \cdot \boldsymbol{K}^s(d^\beta) \cdot \mathbb{M}_2^{vw,\beta}$$

1 / GLRC_HEGIS – SUMMARY

Local mechanism	Internal variables		Thermodynamic force	Yield function
Concrete damage	d		Y	$f_d(Y)$
Concrete cracking	$w_{\gamma,n}$	$\mathrm{w}_\gamma = \begin{pmatrix} w_{\gamma,n} \\ w_{\gamma,t} \end{pmatrix}$	$\underline{q}_{r\gamma}$	$f_{g\gamma n}(q_{r\gamma,n}, w_{\gamma,n}, w_{\gamma,n}^{\max})$
	$w_{\gamma,t}$			$f_{g\gamma t}(q_{r\gamma,t}, w_{\gamma,t})$
Steel-concrete slip	v_x^p	$\mathrm{v}^p = \begin{pmatrix} v_x^p \\ v_y^p \end{pmatrix}$	$\underline{q}_v$	$f_{vx}(q_{v,x}, \underline{w}_1, \underline{w}_2, v_x^p)$
	v_y^p			$f_{vy}(q_{v,y}, \underline{w}_1, \underline{w}_2, v_y^p)$
Steel yielding	ε_x^{ps}	$\varepsilon_{ps} = \begin{pmatrix} \varepsilon_x^{ps} \\ \varepsilon_y^{ps} \end{pmatrix}$	$\underline{q}_s$	$f_{sy}(q_{s,x}, \underline{w}_1, \underline{w}_2, \underline{v}^p)$
	ε_y^{ps}			$f_{sx}(q_{s,y}, \underline{w}_1, \underline{w}_2, \underline{v}^p)$

Summary table of the internal variables of GLRC_HEGIS

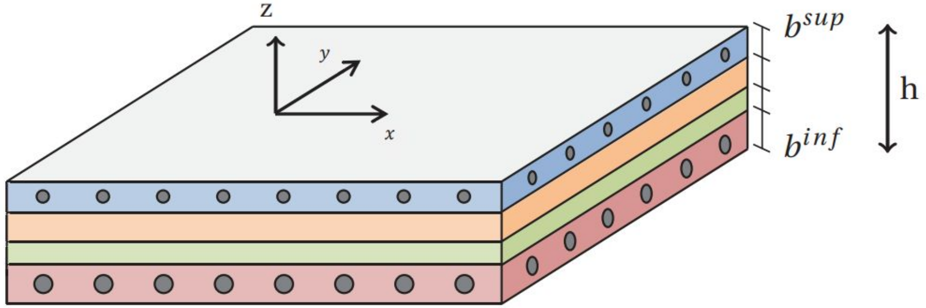

Linear elastic parameters	Section geometry parameters	h	$[m]$	Plate height
		z^β	$[m]$	Position in the Z coordinate of the β steel reinforcement layers
		$A_{s\alpha}^\beta$	$[m]$	Reinforcement section in the α direction of the β layer
	Material elastic properties	E_c	$[Pa]$	Initial (undamaged) concrete Young's modulus
		ν_c	$[-]$	Concrete Poisson's ratio
		$E_{s\alpha}^\beta$	$[Pa]$	Steel Young's modulus
NonLinear parameters	Concrete tensile behaviour	f_{ct}	$[Pa]$	Concrete tensile strength
		G_f	$[N/m]$	Concrete fracture energy
		α_u	$[-]$	Ratio of E_c accounting for the unload slope
		α_r	$[-]$	Ratio of reclosing crack opening over maximum historical crack opening
		$s_{r\alpha}^\beta$	$[m]$	Theoretical average crack spacing in the α direction of the β layer
	Concrete damage parameters	k_o	$[Pa]$	Constant threshold of the energy release rate
		γ_d	$[-]$	Fraction of E_c corresponding to the asymptotic fully damaged concrete slope
	Aggregate interlock	T_o	$[Pa]$	Initial crack shear resistance
		T_1	$[Pa/m]$	Stiffness of the aggregate interlock
	Steel yielding	$f_{sy\alpha}^\beta$	$[Pa]$	Steel yielding stress
	Bond stresses and tension stiffening	K_l	$[Pa/m]$	Initial local bond-slip tangent stiffness
		k_t	$[-]$	Maximum average tension stiffening coefficient in the concrete.
		ϕ_α^β	$[m]$	Diameter of reinforcement bars in the α direction of the β layer

1* : Summary table of geometrical and material parameters of GLRC_HEGIS

GLRC_HEGIS – Mfront : **7** internal variables, i.e. 7 thresholds that can be active at the same time
GLRC_HEGIS : **18** internal variables,

*1 : M. HUGUET, Un modèle global homogénéisé pour la fissuration des voiles en béton armé sous chargements sismiques (2016)

2 / NUMERICAL IMPLEMENTATION – STATUS METHOD

Algorithm: Newton-Raphson with numerical Jacobian
Modelling hypothesis: Plane stress

@Predictor{
- Threshold functions activated ? **(1)**

}
@**Integrator**{
- Resolution if the threshold function was activated

}
@AdditionalConvergenceChecks{
- Checks :
    - Khun-Tucker conditions verified ? **(2)**
    - Final value of internal variable within thresholds ?

}

Implementation difficulties:

- **Many internal variables** ;
- Coupled internal variables = **convergence difficulties**
- **Multiple threshold functions** = **numerous checks** at the end of integratio

➡ **Perform many test cases to verify the validity of the code.**

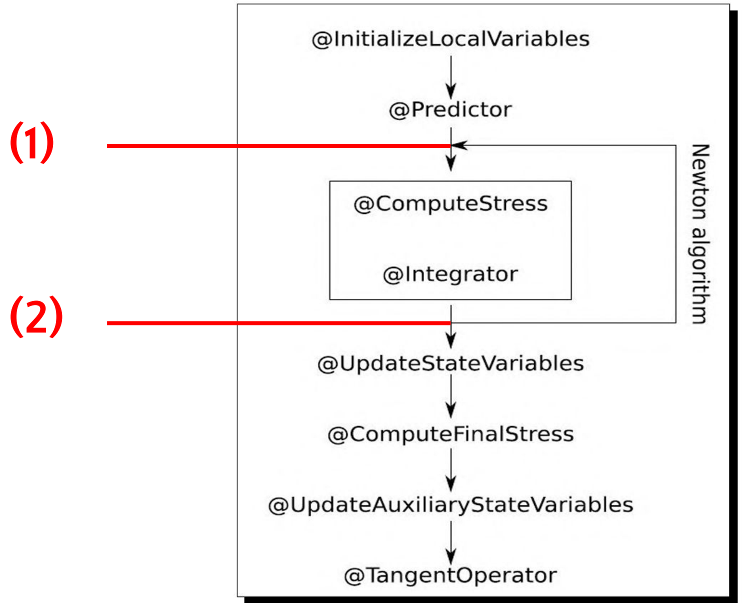

2* : Numerical Integration scheme of MFront

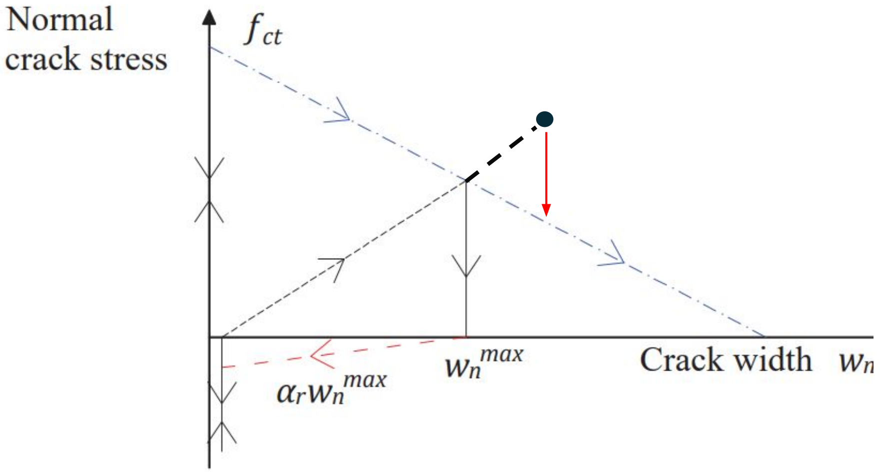

1* : Normal-to crack concrete stress at cracks as a function of crack opening

egis

Data sensitivity - Public

*1 : T.HELFER & al, Le générateur de code Mfront : écriture de lois de comportement mécanique (2013)
*2 : M. HUGUET, Un modèle global homogénéisé pour la fissuration des voiles en béton armé sous chargements sismiques (2016)

2 / NUMERICAL IMPLEMENTATION – COMPATIBILITY DIGITAL COMPATIBILITY OF SHELL ELEMENTS WITH MFRONT

The GLRC_HEGIS constitutive model is initially a generalised shell behaviour, but MFront only works with membrane deformations under plane stresses, so the law must be adapted to switch from single-layer shells to multi-layer plates.

Generalised Single-layer shell (DKTG)	$\underset{\sim}{N} = f(\underset{\sim}{\varepsilon}, \underset{\sim}{\kappa}, \underline{\alpha}) \quad \underset{\sim}{M} = f(\underset{\sim}{\varepsilon}, \underset{\sim}{\kappa}, \underline{\alpha})$

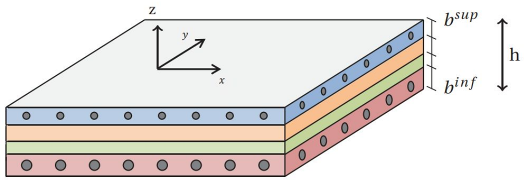

Multilayer shell (DKT)	$\underset{\sim}{\sigma} = f(\underset{\sim}{\varepsilon}, \underline{\alpha})$

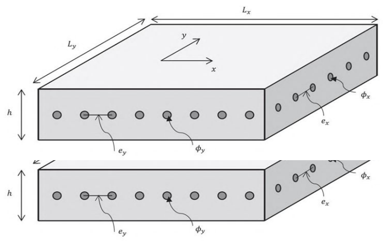

Equivalent membrane behaviour ;

Different bending behaviour in numerical implementation

Some issues with interfaces with MFront for shell elements

*1 : M. HUGUET, Un modèle global homogénéisé pour la fissuration des voiles en béton armé sous chargements sismiques (2016)

3 / RESULTS – BENMANSOUR (CYCLIC TENSION-COMPRESSION LOADING ON RC BEAM

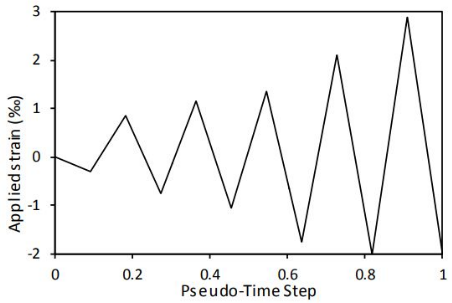

1* Loading of the RC beam

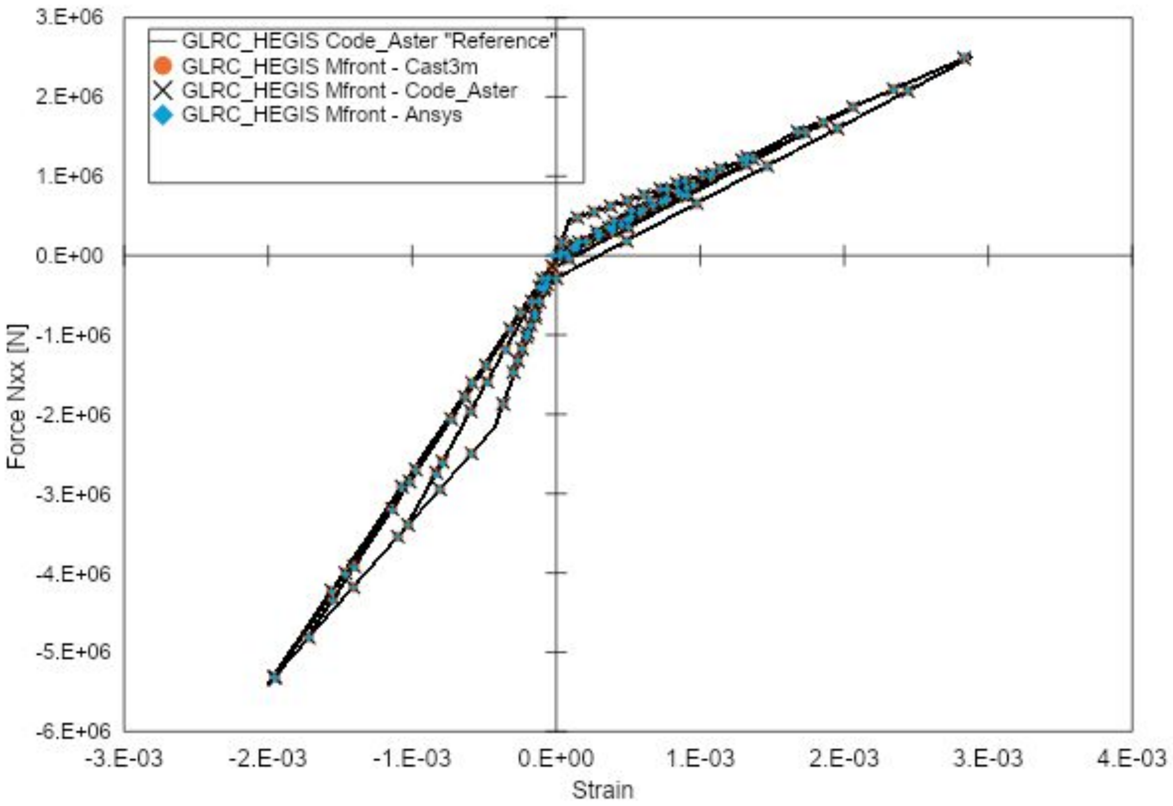

Force–displacement curve comparison: MFront vs. Code_Aster reference

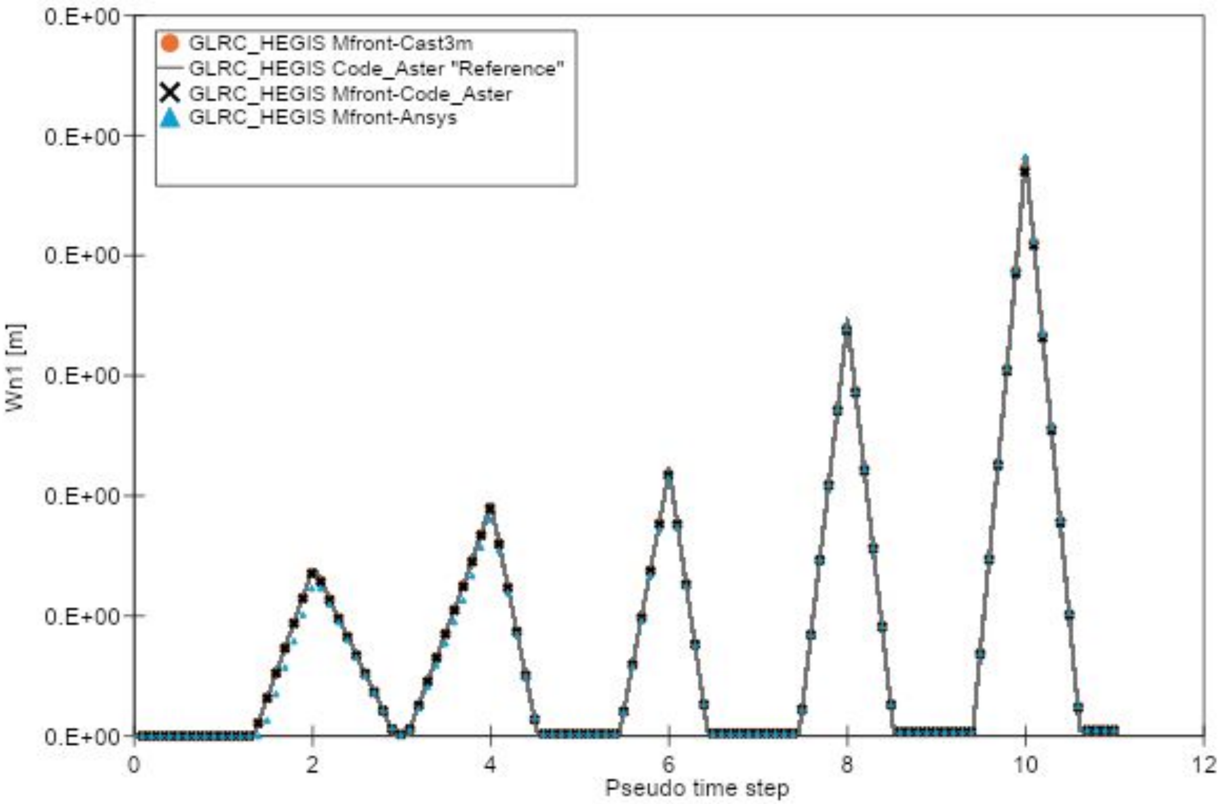

Crack opening–pseudo time curve comparison: MFront vs. Code_Aster reference

Data sensitivity - Public

*1 : M. HUGUET, Un modèle global homogénéisé pour la fissuration des voiles en béton armé sous chargements sismiques (2016)

3 / RESULTS – BENCHMARK SAFE

*1 : Experimental setup diagram of the SAFE benchmark

*2 : Force–displacement curve comparison : GLRC_HEGIS ; GLRC_DM ; EIB ; Experimental

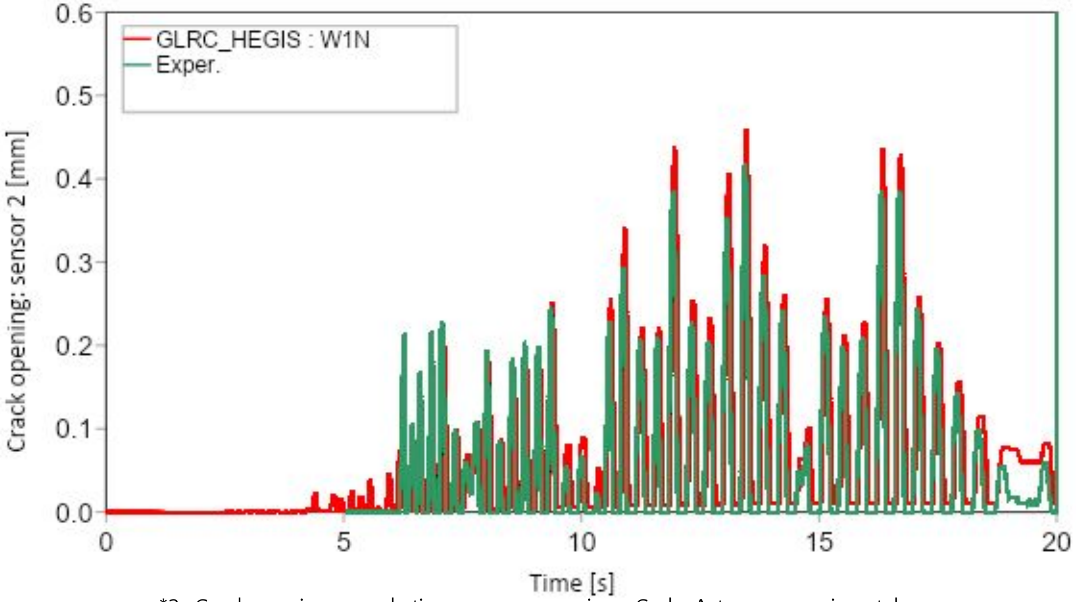

*2 : Crack opening–pseudo time curve comparison: Code_Aster vs. experimental

*1 : Pegon P & al. Programme SAFE: Rapport du test T5. Technical Note, Joint Research Center (1998).
*2 : APPUI À LA RÉDACTION D'UN GUIDE MÉTHODOLOGIQUE RELATIF À L'UTILISATION DE MÉTHODES NON LINÉAIRES POUR L'ANALYSE SISMIQUE DE STRUCTURES DE GÉNIE CIVIL

3 / RESULTS – SAFE

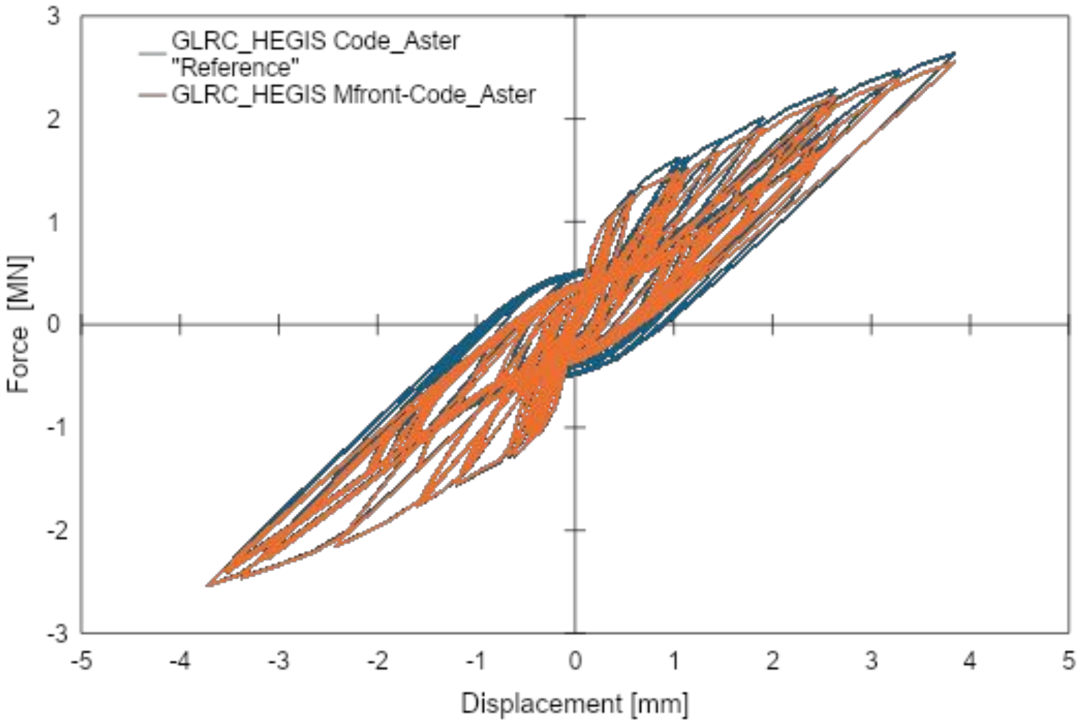

Force–displacement curve comparison: MFront vs. Code_Aster reference

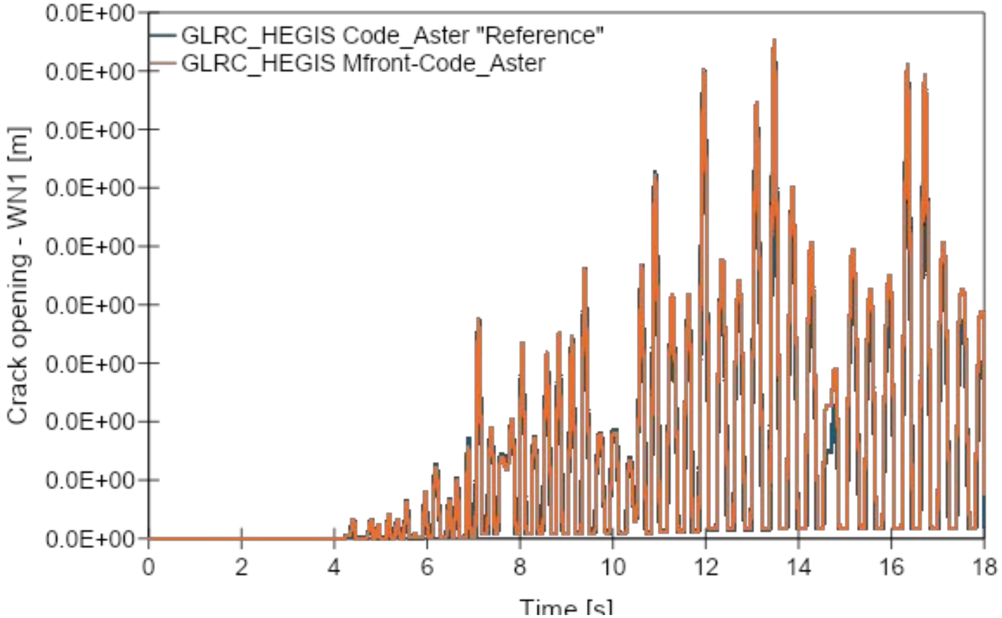

Crack opening (Wn1)–pseudo time curve comparison: MFront vs. Code_Aster reference

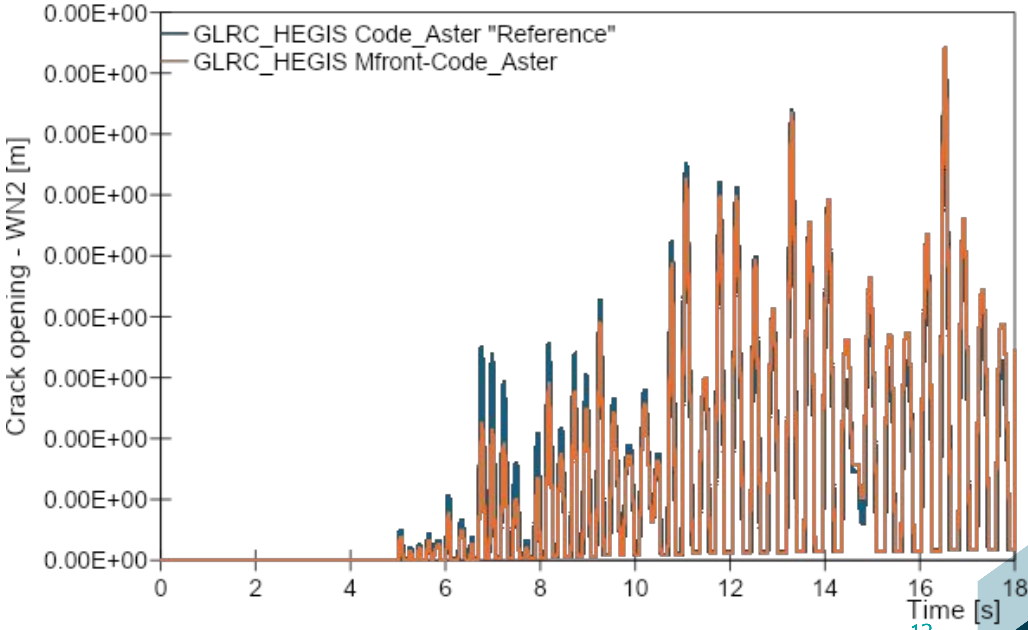

Crack opening (Wn2)–pseudo time curve comparison: MFront vs. Code_Aster reference

- The differences observed appear to stem from an **error in Wn2** ;
- Computing time reduced by a **factor of three** because the time step division is less significant with Mfront.

4 / CONCLUSIONS

- **Consistent results in membrane and bending loading** according to the different solvers used (ANSYS, Code_Aster, Cast3m)
- **Reduced calculation time** compared to the original code on Code_Aster
- Possibility of using the model on other solvers such as ANSYS = **major innovation in the field of civil nuclear power**

- Adaptation of the code required in bending to fully comply with the initial model
- Using shells with MFRONT remains complicated because the interfaces with the solvers contain errors.

Next steps :

- Complete the numerical implementation by correcting errors
- Correct errors at interfaces (Code_Aster)
- Developing digital tools to facilitate the use of the constiutive model

4 / CONCLUSIONS

$$\begin{cases} f_{gn1}(q_{r,n}, w_n, w_n^{\max}) = q_{r,n} - \frac{h_{c1}}{s_r} g_n\left(w_n^{\max}\right) \frac{w_n}{w_n^{\max}} \leq 0 \\ f_{gn2}(q_{r,n}, w_n, w_n^{\max}) = \left(-q_{r,n} - \frac{h_{c1}}{s_r} \alpha_u E_c \frac{w_n^{\max} - w_n}{s_r}\right) H\left(w_n - \alpha_r w_n^{\max}\right) \leq 0 \end{cases}$$

$$f_{s\alpha}\left(q_{s,\alpha}, \underline{w}_1, \underline{w}_2, \underline{v}^p\right) = \left| \frac{q_{s,\alpha}}{\rho_{s\alpha} b} + \left(\boldsymbol{K}^p \cdot \left(\sum_{\gamma} \boldsymbol{M}_{eq}^{vw}(\theta_{r\gamma}) \cdot \underline{w}_{\gamma} - \underline{v}^p \right) \right) \cdot \underline{e}_{\alpha} \right| - f_{sy\alpha} \leq 0$$

$$\underset{\sim}{N} = \frac{\partial \Psi_0}{\partial \underset{\sim}{\varepsilon}} = \underset{\approx}{A}(d) : \underset{\sim}{\varepsilon} - \underset{\approx}{B}'(d, \theta_r) \cdot \underline{w} - \underset{\approx}{C} \cdot \underline{\varepsilon}^{ps}$$

$$Y = -\frac{\partial \Psi_0}{\partial d} = -\frac{1}{2} \underset{\sim}{\varepsilon} : \underset{\approx}{A}'(d) : \underset{\sim}{\varepsilon} + \underset{\sim}{\varepsilon} : \underset{\approx}{B}'(d, \theta_r) \cdot \underline{w} - \frac{1}{2} \underline{w}^T \cdot \underset{\sim}{D}'(d, \theta_r) \cdot \underline{w}$$

$$\underline{q_r} = -\frac{\partial \Psi_0}{\partial \underline{w}} = \underset{\sim}{\varepsilon} : \underset{\approx}{B}(d, \theta_r) - \underset{\sim}{D}(d, \theta_r) \cdot \underline{w} + \underset{\sim}{G}(\theta_r) \cdot \underline{v}^p$$

$$\underline{q_v} = -\frac{\partial \Psi_0}{\partial \underline{v}^p} = \left(\underline{w}^T \cdot \underset{\sim}{G}(\theta_r)\right)^T - \underset{\sim}{E}(\theta_r) \cdot \underline{v}^p$$

$$\underline{q_s} = -\frac{\partial \Psi_0}{\partial \underline{\varepsilon}^{ps}} = \underset{\approx}{C} : \underset{\sim}{\varepsilon} - \underset{\sim}{F} \cdot \underline{\varepsilon}^{ps}$$